JOURNAL OF SPACECRAFT AND ROCKETS
Vol. 44, No. 3, May–June 2007

Thrust Vector Control Analysis and Design for Solar-Sail Spacecraft

Bong Wie*
Arizona State University, Tempe, Arizona 85287-6106

DOI: 10.2514/1.23084

This paper presents a comprehensive mathematical formulation as well as a practical solution of the thrust vector control design problem of solar-sail spacecraft. Thrust vector control logic is part of an attitude and orbit control system of sailcraft, which maintains the proper orientation of a sailcraft to provide its desired thrust vector pointing/steering. The solar-pressure thrust vector direction of a sailcraft is often described by its cone and clock angles measured with respect to certain orbital reference frames. This paper describes various forms of orbital trajectory equations, which employ two different sets of such cone and clock angles, for the analysis, design, and simulation of solar-sail thrust vector control systems. In particular, quaternion-based thrust vector control/orbit control system architecture is proposed for solar sails because of its simple computational algorithm for determining the desired sailcraft attitude quaternions from the commanded cone and clock angles of the solar-pressure thrust vector. The practicality of the proposed quaternion-based thrust vector control/orbit control system architecture is demonstrated for the Solar Polar Imager mission employing a 160-m, 450-kg solar-sail spacecraft.

I. Introduction

SOLAR sails have the potential to provide cost effective, propellantless propulsion that enables longer mission lifetimes, increased scientific payload mass fraction, and access to previously inaccessible orbits (e.g., high solar latitude, retrograde heliocentric, and non-Keplerian) [1–3]. The recent advances in lightweight deployable booms, ultralightweight sail films, and small satellite technologies are spurring a renewed interest in solar sailing and the missions it enables. As a result, near-term solar-sail missions are being developed and the associated sailcraft technologies are rapidly progressing [3–5].

In support of interplanetary solar sailing missions, such as the Comet Halley Rendezvous Mission [1] and the Solar Polar Imager (SPI) Mission,[†] the solar sailing trajectory optimization problem has been extensively studied in the past [6–12]. For typical solar sailing trajectory optimization problems, trajectory models which are decoupled from attitude dynamics were often used in the past. However, the effect of attitude motion of large solar sails on the solar sailing trajectory is of current practical concern for solar-sail mission designs. Consequently, a 6-degree-of-freedom, orbit-attitude coupled dynamical model of solar-sail spacecraft is considered for the solar-sail trajectory optimization and simulation in [13].

This paper is intended to provide a comprehensive mathematical formulation of the thrust vector control (TVC) design problem of a solar-sail spacecraft. As part of an attitude and orbit control system (AOCS) of a sailcraft, a TVC system maintains the proper orientation of the sailcraft to provide the desired thrust vector pointing/steering. The solar-pressure thrust vector direction of the sailcraft is often described by its cone and clock angles measured with respect to certain orbital reference frames such as an osculating orbital reference frame. This paper describes several forms of orbital trajectory equations employing two different sets of such cone and clock angles. In particular, a quaternion-feedback attitude control scheme [14,15] is proposed for an actual TVC system implementation on a solar-sail spacecraft because of its simple interface with the commanded optimal trajectory control inputs. This paper presents a simple computational algorithm for determining the desired sailcraft attitude quaternions from the commanded cone and clock angles of the solar-pressure thrust vector.

Most solar-sail TVC systems, with the inherent inability to precisely model the solar radiation pressure and to accurately point the true thrust vector direction, will require frequent updates of both orbital parameters and TVC steering commands for frequent trajectory corrections [16]. The frequency of such orbit determination and TVC command updates is determined by many factors, such as the trajectory dispersions, the target-body ephemeris uncertainty, the calibration of a solar radiation pressure model, and the operational constraints. Although the solar-sail navigation problem is of practical importance for future solar-sail missions, this paper will focus on the TVC/AOCS design problem assuming that frequent updates of both orbital parameters and TVC steering commands will be provided from a solar-sail navigation and guidance system.

The remainder of this paper is outlined as follows. In Sec. II, various forms of orbital trajectory equations employing two different sets of cone and clock angles are described. Section III presents examples of solar-sail trajectory design and simulation. Section IV describes a quaternion-based TVC/AOCS architecture and a set of the attitude-orbit coupled equations for TVC design and simulation. A TVC/AOCS design example of the SPI mission is described in Sec. V.

II. Solar-Sail Orbital Dynamics

In this section we examine various basic forms of orbital trajectory equations for solar-sail trajectory design and simulation. In general, the orbital equation of a sailcraft in a heliocentric orbit is simply described by

$$\ddot{\boldsymbol{r}} + \frac{\mu}{r^3}\boldsymbol{r} = \boldsymbol{F} + \boldsymbol{G} \tag{1}$$

where $\boldsymbol{r}$ is the position vector of the sailcraft from the center of the sun, $\mu \approx \mu_\odot = 132,715E6\ \mathrm{km}^3/\mathrm{s}^2$, $\boldsymbol{F}$ is the solar radiation

Presented as Paper 6086 at the AIAA Guidance, Navigation, and Control Conference, San Francisco, CA, 15–18 August 2005; received 8 February 2006; revision received 28 November 2006; accepted for publication 29 November 2006.

*Professor, Department of Mechanical and Aerospace Engineering, Mail Code 6106; currently Vance Coffman Endowed Chair Professor, Iowa State University, Department of Aerospace Engineering, 2271 Howe Hall, Room 2355, Ames, IA 50011-2271. Associate Fellow AIAA.

[†]Murphy, N., "Solar Polar Imager Vision Mission Overview," http://lws.gsfc.nasa.gov/solar_sails_conf/NMurphy.pdf [retrieved 22 January 2005].

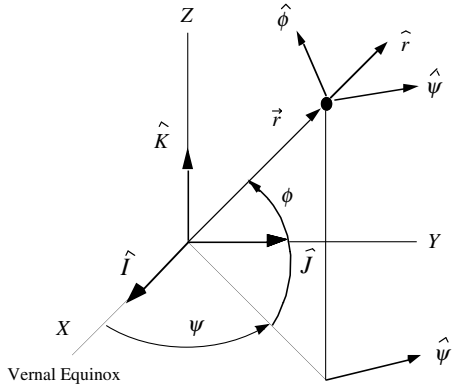

Fig. 1 Heliocentric ecliptic coordinates (X, Y, Z) and spherical coordinates (r, ψ, ϕ).

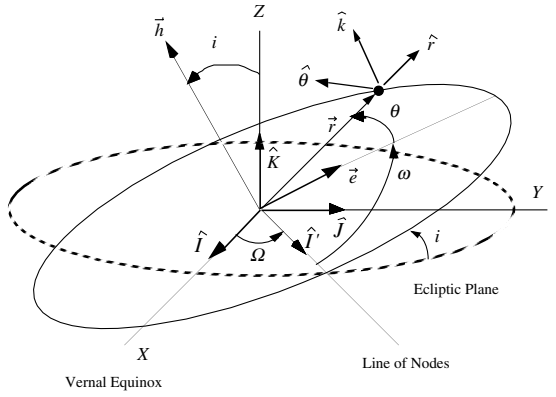

Fig. 3 Orbital geometry (illustrated for a near-circular orbit).

pressure force vector (per unit mass) acting on the sailcraft, and $\boldsymbol{G}$ is the sum of all the perturbing gravitational forces (per unit mass) acting on the sailcraft. In this paper, all the perturbing gravitational forces are ignored without loss of generality.

A. Cone and Clock Angles

The orientation of the solar-sail thrust vector, ideally normal to the sail plane, is often described in terms of the cone and clock angles. These two angles are the typical trajectory control inputs used in solar-sail trajectory optimization. There are at least two different sets of cone/clock angles used in the literature. In this section, the fundamentals of orbital equations of motion in various coordinates employing such two different sets of cone/clock angles are described for the purpose of trajectory design, TVC design, and simulation.

Let $\{\hat{I}, \hat{J}, \hat{K}\}$ and $\{\hat{r}, \hat{\psi}, \hat{\phi}\}$ be, respectively, a set of right-handed, orthonormal vectors of the heliocentric ecliptic rectangular and spherical coordinate reference frames, as illustrated in Fig. 1. These two sets of basis vectors are related as

$$\begin{bmatrix} \hat{r} \\ \hat{\psi} \\ \hat{\phi} \end{bmatrix} = \begin{bmatrix} \cos\phi & 0 & \sin\phi \\ 0 & 1 & 0 \\ -\sin\phi & 0 & \cos\phi \end{bmatrix} \begin{bmatrix} \cos\psi & \sin\psi & 0 \\ -\sin\psi & \cos\psi & 0 \\ 0 & 0 & 1 \end{bmatrix} \begin{bmatrix} \hat{I} \\ \hat{J} \\ \hat{K} \end{bmatrix} \tag{2}$$

where ψ and ϕ are called the ecliptic longitude and latitude of the sailcraft position, respectively; $0 \le \psi \le 360$ deg and $-90 \le \phi \le +90$ deg.

The sailcraft position vector is then expressed as

$$\begin{aligned} \boldsymbol{r} &= r\hat{r} = (r\cos\phi\cos\psi)\hat{I} + (r\cos\phi\sin\psi)\hat{J} + (r\sin\phi)\hat{K} \\ &= X\hat{I} + Y\hat{J} + Z\hat{K} \end{aligned} \tag{3}$$

where $r = |\boldsymbol{r}|$ is the distance from the sun to the sailcraft.

The orientation of a unit vector normal to the sail plane $\hat{n}$ is described in terms of the cone angle α and the clock angle β, illustrated in Fig. 2, as follows:

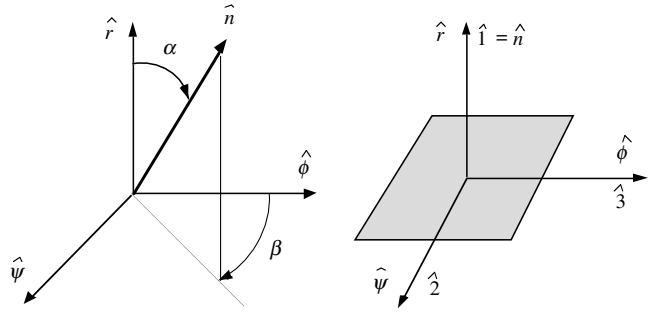

Fig. 2 Cone angle α, clock angle β, and sailcraft orientation when $\alpha = \beta = 0$.

$$\hat{n} = (\cos\alpha)\hat{r} + (\sin\alpha\sin\beta)\hat{\psi} + (\sin\alpha\cos\beta)\hat{\phi} \tag{4}$$

where

$$\cos\alpha = \hat{r}\cdot\hat{n} \qquad \cos\beta = \frac{\hat{r}\times(\hat{n}\times\hat{r})}{|\hat{r}\times(\hat{n}\times\hat{r})|}\cdot\hat{\phi} \qquad 0 \le \alpha \le 90 \text{ deg}$$
$$0 \le \beta \le 360 \text{ deg}$$

As also illustrated in Fig. 2, the sailcraft body-fixed basis vectors $\{\hat{1}, \hat{2}, \hat{3}\}$ are assumed to be aligned with $\{\hat{r}, \hat{\psi}, \hat{\phi}\}$ when $\alpha = \beta = 0$, and the sailcraft roll axis is defined to be perpendicular to the sail surface; that is, $\hat{1} \equiv \hat{n}$. The sailcraft body-fixed basis vectors $\{\hat{1}, \hat{2}, \hat{3}\}$ are then related to $\{\hat{r}, \hat{\psi}, \hat{\phi}\}$ as follows:

$$\begin{bmatrix} \hat{1} \\ \hat{2} \\ \hat{3} \end{bmatrix} = \begin{bmatrix} \cos\alpha & 0 & \sin\alpha \\ 0 & 1 & 0 \\ -\sin\alpha & 0 & \cos\alpha \end{bmatrix} \begin{bmatrix} 1 & 0 & 0 \\ 0 & \cos\beta & -\sin\beta \\ 0 & \sin\beta & \cos\beta \end{bmatrix} \begin{bmatrix} \hat{r} \\ \hat{\psi} \\ \hat{\phi} \end{bmatrix} \tag{5}$$

Let $\{\hat{r}, \hat{\theta}, \hat{k}\}$ be a set of basis vectors of an osculating orbital plane, as illustrated in Fig. 3. A different set of the cone and clock angles (α, δ) can then be defined as shown in Fig. 4. A body-fixed rotational sequence to $\{\hat{1}, \hat{2}, \hat{3}\}$ from $\{\hat{I}, \hat{J}, \hat{K}\}$ is then described by successive coordinate transformations of the form [17]

$$\mathbf{C}_2(-\alpha) \leftarrow \mathbf{C}_1(-\delta) \leftarrow \mathbf{C}_3(\theta) \leftarrow \mathbf{C}_3(\omega) \leftarrow \mathbf{C}_1(i) \leftarrow \mathbf{C}_3(\Omega)$$

which becomes

$$\begin{bmatrix} \hat{r} \\ \hat{\theta} \\ \hat{k} \end{bmatrix} = \begin{bmatrix} \cos(\omega+\theta) & \sin(\omega+\theta) & 0 \\ -\sin(\omega+\theta) & \cos(\omega+\theta) & 0 \\ 0 & 0 & 1 \end{bmatrix} \begin{bmatrix} 1 & 0 & 0 \\ 0 & \cos i & \sin i \\ 0 & -\sin i & \cos i \end{bmatrix} \times \begin{bmatrix} \cos\Omega & \sin\Omega & 0 \\ -\sin\Omega & \cos\Omega & 0 \\ 0 & 0 & 1 \end{bmatrix} \begin{bmatrix} \hat{I} \\ \hat{J} \\ \hat{K} \end{bmatrix} \tag{6}$$

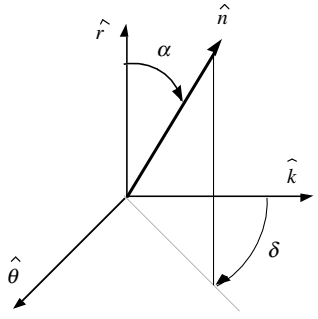

Fig. 4 Cone angle α and clock angle δ [2].

$$\begin{bmatrix}\hat{1}\\ \hat{2}\\ \hat{3}\end{bmatrix}=\begin{bmatrix}\cos\alpha & 0 & \sin\alpha\\ 0 & 1 & 0\\ -\sin\alpha & 0 & \cos\alpha\end{bmatrix}\begin{bmatrix}1 & 0 & 0\\ 0 & \cos\delta & -\sin\delta\\ 0 & \sin\delta & \cos\delta\end{bmatrix}\begin{bmatrix}\hat{r}\\ \hat{\theta}\\ \hat{k}\end{bmatrix} \quad (7)$$

The orientation of a unit vector normal to the sail plane $\hat{n}$ is then described in terms of α and δ, as illustrated in Fig. 4, as follows:

$$\hat{n}=(\cos\alpha)\hat{r}+(\sin\alpha\sin\delta)\hat{\theta}+(\sin\alpha\cos\delta)\hat{k} \quad (8)$$

and

$$\cos\alpha=\hat{r}\cdot\hat{n} \qquad \cos\delta=\frac{\hat{r}\times(\hat{n}\times\hat{r})}{|\hat{r}\times(\hat{n}\times\hat{r})|}\cdot\hat{k} \qquad 0\le\alpha\le 90 \text{ deg}$$
$$0\le\delta\le 360 \text{ deg}$$

B. Solar Radiation Pressure

An ideal model of the solar radiation pressure (SRP) is used here. The SRP force vector (per unit mass) acting on the sailcraft is described in various coordinates as follows:

$$\boldsymbol{F}=F_0(\hat{r}\cdot\hat{n})^2\hat{n}=F_r\hat{r}+F_\psi\hat{\psi}+F_\phi\hat{\phi}=R\hat{r}+T\hat{\theta}+N\hat{k}$$
$$=F_X\hat{I}+F_Y\hat{J}+F_Z\hat{K} \quad (9)$$

where

$$F_0=\left(\frac{r_\oplus}{r}\right)^2 a_c \quad (10)$$

where $r_\oplus=1$ AU $=149,597,870.691$ km is the distance from the sun to the Earth and a_c is the so-called characteristic acceleration of the sailcraft at 1 AU.

Furthermore, we have the following relationships:

$$\begin{bmatrix}F_r\\ F_\psi\\ F_\phi\end{bmatrix}=F_0\cos^2\alpha\begin{bmatrix}\cos\alpha\\ \sin\alpha\sin\beta\\ \sin\alpha\cos\beta\end{bmatrix} \quad (11)$$

$$\begin{bmatrix}R\\ T\\ N\end{bmatrix}=F_0\cos^2\alpha\begin{bmatrix}\cos\alpha\\ \sin\alpha\sin\delta\\ \sin\alpha\cos\delta\end{bmatrix} \quad (12)$$

$$\begin{bmatrix}F_r\\ F_\psi\\ F_\phi\end{bmatrix}=\begin{bmatrix}\cos\phi & 0 & \sin\phi\\ 0 & 1 & 0\\ -\sin\phi & 0 & \cos\phi\end{bmatrix}\begin{bmatrix}\cos\psi & \sin\psi & 0\\ -\sin\psi & \cos\psi & 0\\ 0 & 0 & 1\end{bmatrix}\begin{bmatrix}F_X\\ F_Y\\ F_Z\end{bmatrix} \quad (13)$$

$$\begin{bmatrix}R\\ T\\ N\end{bmatrix}=\begin{bmatrix}\cos(\omega+\theta) & \sin(\omega+\theta) & 0\\ -\sin(\omega+\theta) & \cos(\omega+\theta) & 0\\ 0 & 0 & 1\end{bmatrix}\begin{bmatrix}1 & 0 & 0\\ 0 & \cos i & \sin i\\ 0 & -\sin i & \cos i\end{bmatrix}$$
$$\times\begin{bmatrix}\cos\Omega & \sin\Omega & 0\\ -\sin\Omega & \cos\Omega & 0\\ 0 & 0 & 1\end{bmatrix}\begin{bmatrix}F_X\\ F_Y\\ F_Z\end{bmatrix} \quad (14)$$

C. Orbital Equations in Rectangular Coordinates

The orbital equation of motion in vector form, Eq. (1), can be expressed in the rectangular coordinates as follows:

$$\ddot{X}=-\frac{\mu X}{r^3}+F_X \quad (15a)$$

$$\ddot{Y}=-\frac{\mu Y}{r^3}+F_Y \quad (15b)$$

$$\ddot{Z}=-\frac{\mu Z}{r^3}+F_Z \quad (15c)$$

where $r=\sqrt{X^2+Y^2+Z^2}$ and

$$\begin{bmatrix}F_X\\ F_Y\\ F_Z\end{bmatrix}=\begin{bmatrix}\cos\psi & -\sin\psi & 0\\ \sin\psi & \cos\psi & 0\\ 0 & 0 & 1\end{bmatrix}\begin{bmatrix}\cos\phi & 0 & -\sin\phi\\ 0 & 1 & 0\\ \sin\phi & 0 & \cos\phi\end{bmatrix}\begin{bmatrix}F_r\\ F_\psi\\ F_\phi\end{bmatrix} \quad (16)$$

$$\sin\psi=\frac{Y}{\sqrt{X^2+Y^2}}; \qquad \cos\psi=\frac{X}{\sqrt{X^2+Y^2}} \qquad \sin\phi=\frac{Z}{r}$$
$$\cos\phi=\frac{\sqrt{X^2+Y^2}}{r}$$

When the orientation of $\hat{n}$ is described in terms of α and δ, as shown in Fig. 4, we use the following coordinate transformation:

$$\begin{bmatrix}F_X\\ F_Y\\ F_Z\end{bmatrix}=\begin{bmatrix}\cos\Omega & -\sin\Omega & 0\\ \sin\Omega & \cos\Omega & 0\\ 0 & 0 & 1\end{bmatrix}\begin{bmatrix}1 & 0 & 0\\ 0 & \cos i & -\sin i\\ 0 & \sin i & \cos i\end{bmatrix}$$
$$\times\begin{bmatrix}\cos(\omega+\theta) & -\sin(\omega+\theta) & 0\\ \sin(\omega+\theta) & \cos(\omega+\theta) & 0\\ 0 & 0 & 1\end{bmatrix}\begin{bmatrix}R\\ T\\ N\end{bmatrix}$$

For this case of employing (R,T,N), we need to determine (Ω,i,ω,θ) for given $(X,Y,Z,\dot{X},\dot{Y},\dot{Z})$.

The six classical orbital elements (a,e,i,Ω,ω,M) can be determined for given $\boldsymbol{r}=X\boldsymbol{I}+Y\boldsymbol{J}+Z\boldsymbol{K}$ and $\boldsymbol{v}=\dot{X}\boldsymbol{I}+\dot{Y}\boldsymbol{J}+\dot{Z}\boldsymbol{K}$, as discussed in Ref. [17].

D. Orbital Equations in Spherical Coordinates

The orbital equations of motion in the spherical coordinates (r,ψ,ϕ) are given by

$$\ddot{r}-r\dot{\phi}^2-r\dot{\psi}^2\cos^2\phi=-\frac{\mu}{r^2}+F_r \quad (17a)$$

$$r\ddot{\psi}\cos\phi+2\dot{r}\,\dot{\psi}\cos\phi-2r\dot{\psi}\,\dot{\phi}\sin\phi=F_\psi \quad (17b)$$

$$r\ddot{\phi}+2\dot{r}\,\dot{\phi}+r\dot{\psi}^2\sin\phi\cos\phi=F_\phi \quad (17c)$$

Let $v_r=\dot{r}$, $v_\psi=r\dot{\psi}\cos\phi$, and $v_\phi=r\dot{\phi}$, then we obtain

$$\dot{r}=v_r \quad (18a)$$

$$\dot{\psi}=\frac{1}{r\cos\phi}v_\psi \quad (18b)$$

$$\dot{\phi}=\frac{1}{r}v_\phi \quad (18c)$$

$$\dot{v}_r=\frac{1}{r}(v_\psi^2+v_\phi^2)-\frac{\mu}{r^2}+F_0\cos^3\alpha \quad (18d)$$

$$\dot{v}_{\psi} = \frac{1}{r}(v_{\psi}v_{\phi}\tan\phi - v_r v_{\psi}) + F_0\cos^2\alpha\sin\alpha\sin\beta \tag{18e}$$

$$\dot{v}_{\phi} = -\frac{1}{r}(v_{\psi}^2\tan\phi + v_r v_{\phi}) + F_0\cos^2\alpha\sin\alpha\cos\beta \tag{18f}$$

where

$$F_0 = \left(\frac{r_{\oplus}}{r}\right)^2 a_c$$

This set of six trajectory equations is often employed to find the time histories of optimal control inputs (α, β). By numerically integrating this set of trajectory equations for known time histories of (α, β), we may obtain $(X, Y, Z, \dot{X}, \dot{Y}, \dot{Z})$ as follows:

$$X = r\cos\phi\cos\psi \tag{19a}$$

$$Y = r\cos\phi\sin\psi \tag{19b}$$

$$Z = r\sin\phi \tag{19c}$$

$$\begin{bmatrix}\dot{X}\\ \dot{Y}\\ \dot{Z}\end{bmatrix} = \begin{bmatrix}\cos\phi\cos\psi & -r\cos\phi\sin\psi & -r\sin\phi\cos\psi\\ \cos\phi\sin\psi & r\cos\phi\cos\psi & -r\sin\phi\sin\psi\\ \sin\phi & 0 & r\cos\phi\end{bmatrix}\begin{bmatrix}\dot{r}\\ \dot{\psi}\\ \dot{\phi}\end{bmatrix} \tag{20}$$

An interesting case of applying the orbital equations of motion expressed in spherical coordinates is the logarithmic spiral trajectory problem [2,18]. Although such logarithmic spiral trajectories are not practically useful for an interplanetary transfer between circular orbits, a simple steering law with a fixed sun angle is required.

For a simple planar case with $\phi = 0$ and $\beta = 0$, we have

$$\ddot{r} - r\dot{\psi}^2 = -\frac{\mu}{r^2} + F_0\cos^3\alpha \tag{21a}$$

$$r\ddot{\psi} + 2\dot{r}\,\dot{\psi} = F_0\cos^2\alpha\sin\alpha \tag{21b}$$

where

$$F_0 = \left(\frac{r_{\oplus}}{r}\right)^2 a_c$$

For this planar case, α is often called a pitch angle with $-90 \le \alpha \le 90$ deg.

By defining a sailcraft lightness number λ as

$$\lambda = \frac{F_0}{\mu/r^2} = \frac{r_{\oplus}^2 a_c}{\mu} = \frac{(149,597,870E3)^2}{132,715E15}a_c = 168.6284a_c \tag{22}$$

we rewrite the orbital equations of motion as

$$\ddot{r} - r\dot{\psi}^2 = -(1-\lambda)\frac{\mu}{r^2}\cos^3\alpha \tag{23a}$$

$$r\ddot{\psi} + 2\dot{r}\,\dot{\psi} = \lambda\frac{\mu}{r^2}\cos^2\alpha\sin\alpha \tag{23b}$$

E. Gauss's Form of the Variational Equations (Osculating Orbital Elements)

A set of six first-order differential equations, called Gauss's form of the variational equations, in terms of osculating orbital elements, are given by [19]

$$\dot{a} = \frac{2a^2}{h}[eR\sin\theta + T(1+e\cos\theta)] \equiv \frac{2a^2}{h}\left[eR\sin\theta + \frac{pT}{r}\right] \tag{24a}$$

$$\dot{e} = \sqrt{\frac{p}{\mu}}[R\sin\theta + T(\cos\theta + \cos E)] \equiv \frac{1}{h}\{pR\sin\theta + [(p+r)\cos\theta + re]T\} \tag{24b}$$

$$\dot{i} = \frac{r\cos(\omega+\theta)}{h}N \tag{24c}$$

$$\dot{\Omega} = \frac{r\sin(\omega+\theta)}{h\sin i}N \tag{24d}$$

$$\dot{\omega} = -\frac{r\sin(\omega+\theta)}{h\tan i}N + \frac{1}{eh}[-pR\cos\theta + (p+r)T\sin\theta] \tag{24e}$$

$$\dot{\theta} = \frac{h}{r^2} + \frac{1}{eh}[pR\cos\theta - (p+r)T\sin\theta] \tag{24f}$$

where

$$p = a(1-e^2)$$

$$r = \frac{p}{1+e\cos\theta} \equiv a(1-e\cos E)$$

$$h = \sqrt{\mu p} = na^2\sqrt{1-e^2}$$

$$n = \sqrt{\mu/a^3}$$

$$\begin{bmatrix}R\\ T\\ N\end{bmatrix} = F_0\cos^2\alpha\begin{bmatrix}\cos\alpha\\ \sin\alpha\sin\delta\\ \sin\alpha\cos\delta\end{bmatrix}$$

$$F_0 = \left(\frac{r_{\oplus}}{r}\right)^2 a_c$$

In particular, the inclination equation becomes

$$\dot{i} = \frac{r\cos(\omega+\theta)}{h}N = \frac{\lambda}{r}\sqrt{\frac{\mu}{p}}\cos^2\alpha\sin\alpha\cos\delta\cos(\omega+\theta) \tag{25}$$

We then obtain a simple sail-steering law for maximizing the rate of change of inclination as

$$\alpha = \tan^{-1}(1/\sqrt{2}) = 35.26 \text{ deg}$$

and

$$\delta = \begin{cases} 0 \text{ deg} & \text{for } \cos(\omega + \theta) \geq 0 \\ 180 \text{ deg} & \text{for } \cos(\omega + \theta) < 0 \end{cases}$$

Although this simple steering law indicates that the clock angle has to change ± 180 deg instantaneously, an equivalent attitude motion is a ± 70- deg single-axis slew maneuver every half orbit (i.e., at ascending and descending nodes). Furthermore, this simple steering law demonstrates an advantage of employing (α, δ) instead of (α, β) because (α, δ) is more conveniently tied to the classical orbital elements.

III. Examples of Solar Sailing Trajectory Design and Simulation

A. Solar Polar Imager Mission

Solar sails are envisioned as a propellantless, high-energy propulsion system for future space exploration missions. NASA's future missions enabled by solar-sail propulsion include the SPI, L1-Diamond, Particle Acceleration Solar Orbiter (PASO), and Interstellar Probe, which are the sun–Earth connections (SEC) solar-sail road map missions [3]. In particular, the SPI mission is currently being further studied by NASA/JPL.[‡] Our current understanding of the sun is limited by a lack of observations of its polar regions. The SPI mission uses a large solar sail to place a spacecraft in a 0.48-AU heliocentric circular orbit with an inclination of 75 deg. Viewing of the polar regions of the sun provides a unique opportunity to more fully investigate the structure and dynamics of its interior, the generation of solar magnetic fields, the origin of the solar cycle, the causes of solar activity, and the structure and dynamics of the corona.

The SPI mission consists of the initial cruise phase to a 0.48-AU circular orbit, the cranking orbit phase, and the science mission phase. A 160-m, 450-kg solar-sail spacecraft is considered as a reference model for such a solar sailing mission. A Delta II launch vehicle is able to inject the 450-kg SPI spacecraft into an Earth escaping orbit with $C_3 = 0.25$ km^2/s^2. The solar sail is to be deployed at the beginning of the interplanetary cruise phase. The SPI sailcraft first spirals inwards from 1 AU to a heliocentric circular orbit at 0.48 AU, then the cranking orbit phase begins to achieve a 75-deg inclination. The solar sail will be jettisoned after achieving the science mission orbit, and the total sailing time is approximately 6.6 years.

Figure 5 shows an optimization-based trajectory design by Carl Sauer at NASA/JPL for achieving a circular orbit at 0.48 AU with a 75-deg inclination. A set of the cone and clock angles, (α, β), was used by Sauer for such a baseline SPI mission trajectory design. The monotonically decreasing semimajor axis and the corresponding variation of eccentricity can be seen in this figure during the initial cruise phase to 0.48 AU. The eccentricity remains constant during the orbit cranking phase. The eccentricity is finally nulled after cranking is complete. A somewhat complicated nature of the desired, optimal clock angle β command can be noticed in Fig. 5, although the cone angle is nearly kept constant except for the final orbit correction phase to null the eccentricity.

A possibility of employing simple sail-steering laws (a combination of constant cone/clock angles), based on Gauss's form of the variational equations with the cone and clock angles (α, δ), was examined for the SPI mission. Figure 6 shows the result of applying such simple sail-steering laws with (α, δ) to the SPI mission. The switch from orbit radius reduction to the cranking phase occurs once the sail reaches the target semimajor axis of 0.48 AU. However, an actual transition to the cranking orbit phase was executed at a proper orbital location such that the large eccentricity variation of the initial cruise phase can be removed as can be seen in Fig. 6. The simulation used a nominal characteristic acceleration of 0.3 mm/s^2 (at 1 AU), an 8-deg initial inclination, and $C_3 = 0.25$ km^2/s^2. The sailcraft

[‡]Murphy, N., "Solar Polar Imager Vision Mission Overview," http://lws.gsfc.nasa.gov/solar_sails_conf/NMurphy.pdf.

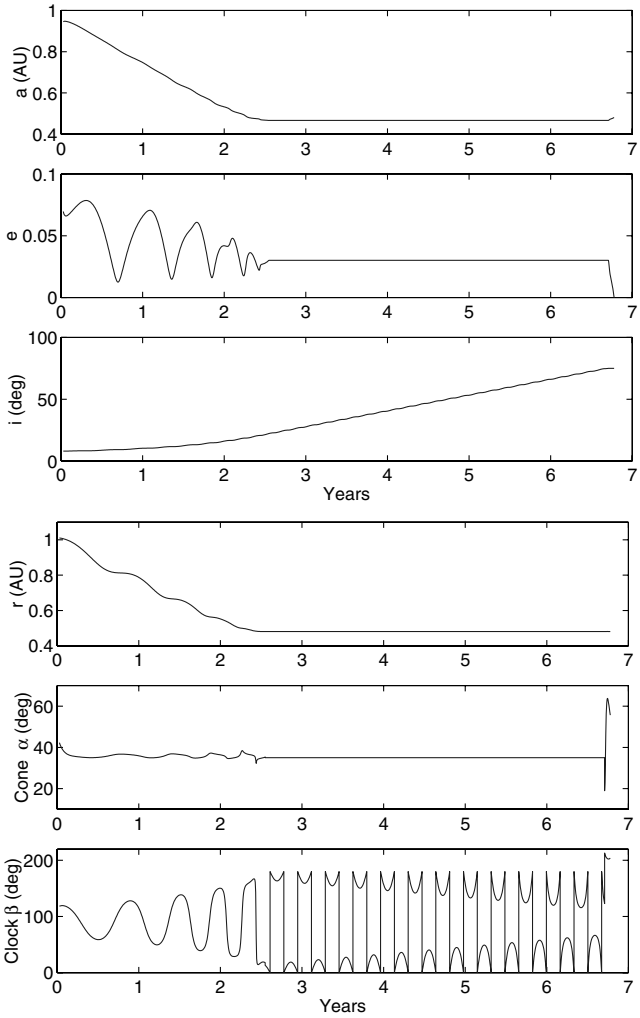

Fig. 5 Optimization-based trajectory design with (α, β) for the SPI mission (Carl Sauer, NASA/JPL).

achieves the desired semimajor axis and inclination but the final orbit is slightly eccentric. The corresponding three-dimensional orbital trajectory is illustrated in Fig. 7.

A comparison of the desired clock-angle commands β and δ, shown in Figs. 5 and 6 respectively, suggests that the clock angle δ is a better choice for an actual TVC steering command implementation because of its simplicity. Another example of using the clock angle δ will be presented in the next section.

B. Solar Sailing Kinetic Energy Impactor (KEI) Mission

A fictional asteroid mitigation problem was created by AIAA for the 2004/2005 AIAA Foundation Undergraduate Team Space Design Competition. A similar fictional asteroid mitigation problem, called the defined threat (DEFT) scenarios, has been created also for the 2004 Planetary Defense Conference. One of the four DEFT scenarios is about mitigating a fictional 200-m Athos asteroid with the predicted impact date of 29 February 2016.

The fictional asteroid mitigation problem of AIAA is briefly described as follows. On 4 July 2004, NASA/JPL's near-Earth asteroid tracking (NEAT) camera at the Maui space surveillance site discovered a 0.205-km diameter Apollo asteroid designated 2004WR. This asteroid has been assigned a torino impact scale rating of 9.0 on the basis of subsequent observations that indicate there is a 95% probability that 2004WR will impact the Earth. The expected impact will occur in the southern hemisphere on 14 January 2015 causing catastrophic damage throughout the Pacific region. The mission is to design a space system that can rendezvous with 2004WR in a timely manner, inspect it, and remove the hazard to Earth by changing its orbit and/or destroying it. The classical

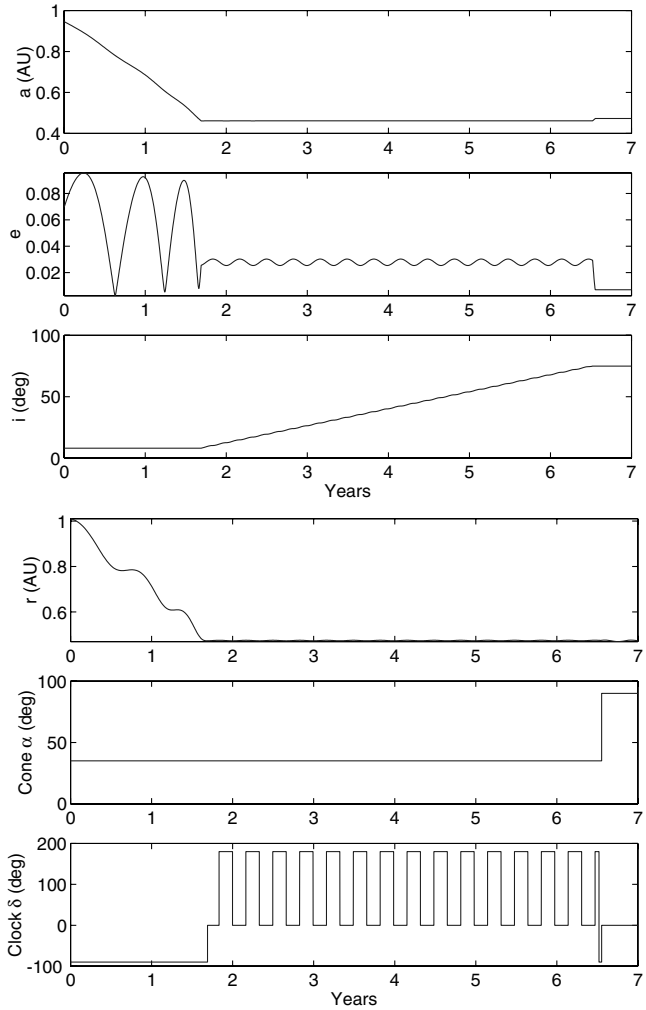

Fig. 6 SPI mission trajectory design using simple sail-steering laws with (α, δ).

orbital elements of 2004WR are given in the J2000 heliocentric ecliptic reference frame as follows:

$$\text{Epoch} = 53200 \text{ TDB (14 July 2004)}$$

$$a = 2.15374076 \text{ AU}$$

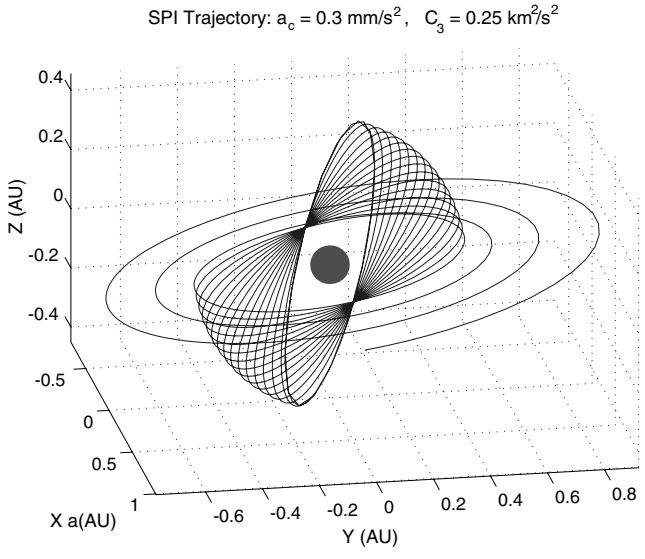

Fig. 7 SPI mission trajectory design result using (α, δ).

$$e = 0.649820926$$

$$i = 11.6660258 \text{ deg}$$

$$\omega = 66.2021796 \text{ deg}$$

$$\Omega = 114.4749665 \text{ deg}$$

$$M = 229.8987151 \text{ deg}$$

The STK 5.0.4 software package, with a 9th-order Runge–Kutta integrator with variable step size and the planetary positions from JPL's DE405, was used by AIAA to create this set of orbital parameters of 2004WR.

It is further assumed that 2004WR is an S-class (stony–silicate) asteroid with a density of 2720 kg/m^3 and that its estimated mass is 1.1×10^{10} kg. If 2004WR is an M-class (nickel–iron) asteroid, then its estimated mass would be 2.2×10^{10} kg.

A solar sailing KEI mission concept applied to the fictional asteroid mitigation problem of AIAA is illustrated in Fig. 8. The proposed mission requires at least ten 160-m, 300-kg solar-sail spacecraft with a characteristic acceleration of 0.5 mm/s^2, as proposed in [20,21] as a viable near-term option for mitigating the threat posed by near-Earth asteroids (NEAs). The solar sailing phase of the proposed KEI mission, which is very similar to that of the SPI mission, is composed of the initial cruise phase from 1 to 0.25 AU, the cranking orbit phase (for a 168-deg inclination change), and the final retrograde orbit phase before impacting the target asteroid at its perihelion with an impact speed larger than 70 km/s.

Simple sail-steering laws based on Gauss's form of the variational equations with the cone and clock angles (α, δ) were examined for the preliminary KEI mission design. Figure 9 shows the result of applying the simple sail-steering laws to the KEI mission. More rigorous trajectory optimization study results for the KEI mission can be found in [21]. In practice, the KEI mission will require precision navigation and guidance, and thus it will require frequent updates of the TVC steering commands.

IV. Solar-Sail Attitude Dynamics and Control

As described in the preceding sections, various forms of orbital trajectory equations employing two sets of the cone and clock angles

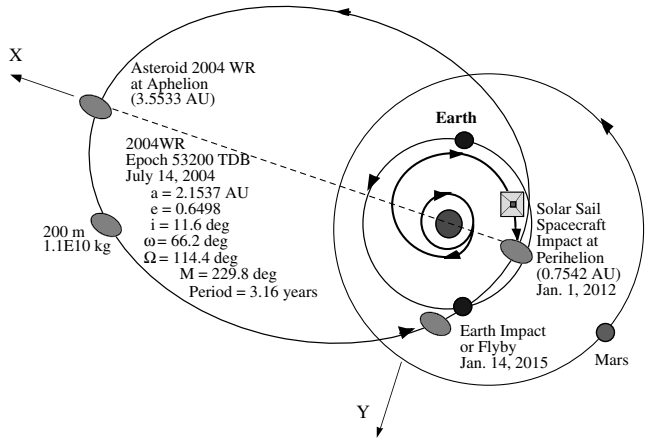

Fig. 8 Illustration of the solar sailing KEI mission for impacting and deflecting a near-Earth asteroid. The final, retrograde heliocentric orbit phase (starting from 0.25 AU) results in a head-on collision with the target asteroid at its perihelion (0.75 AU) with an impact speed larger than 70 km/s.

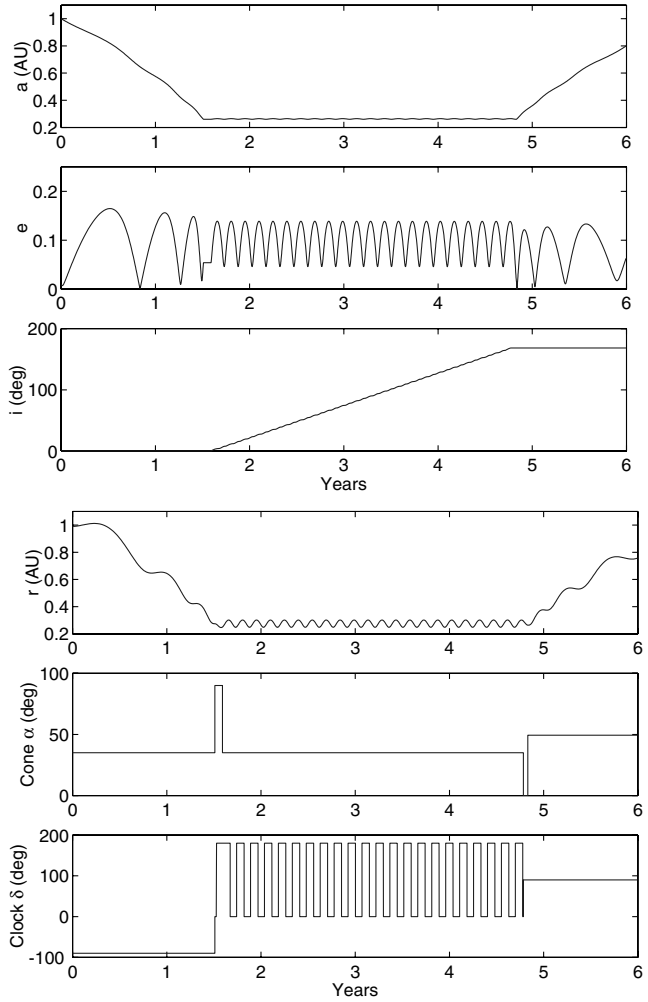

Fig. 9 KEI trajectory design using simple sail-steering laws [20].

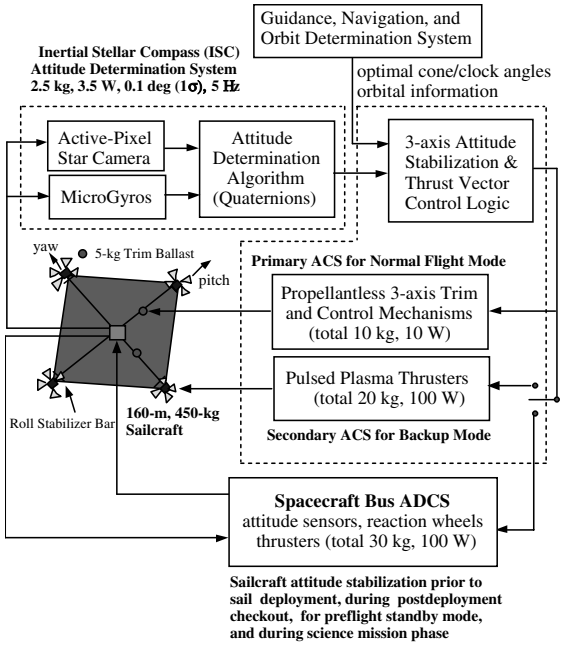

Fig. 10 An integrated TVC/AOCS architecture proposed for the SPI mission.

are available for the solar-sail trajectory design and simulation. It was shown that a preliminary trajectory design can be easily performed by employing simple sail-steering laws as applied to a set of orbital equations, called Gauss's form of the variational equations with (α, δ).

In this section a quaternion-feedback attitude control scheme, previously developed in [14,15], is proposed for solar-sail TVC applications because of its simple interface with the typical trajectory control inputs (the desired cone and clock angles of the solar thrust vector). The practicality and simplicity of the proposed TVC approach will be demonstrated in this section.

A. Solar-Sail TVC/AOCS Architecture

One method of properly controlling the attitude of a large sailcraft is to employ small reflective control vanes mounted at the spar tips. Another method is to change the center-of-mass location relative to its center-of-pressure location. This can be achieved by articulating a control boom with a tip-mounted payload/bus. Various dynamical models and attitude control systems of solar sails, using passive stabilization, spin stabilization, control vanes, a 2-axis gimbaled control boom, or translating/tilting sail panels, can be found in [22].

A baseline TVC/AOCS architecture illustrated in Fig. 10, consisting of a propellantless primary attitude control system (ACS) and a microthruster-based secondary ACS, is proposed for a 160-m sailcraft of the SPI mission as well as the KEI mission. As illustrated in Fig. 11, the primary ACS employs trim control masses (TCMs) running along mast lanyards for pitch/yaw control together with roll stabilizer bars (RSBs) at the mast tips for quadrant tilt control. The robustness of such a propellantless primary ACS would be further enhanced by a backup ACS using tip-mounted, lightweight pulsed plasma thrusters (PPTs). Such a micro-PPT-based ACS can be employed for attitude recovery maneuvers from off-nominal conditions as well as for a spin-stabilized safe mode. It can also be employed as a backup to the conventional bus ACS before sail deployment and during preflight sail checkout operation, if necessary. A conventional bus ACS is required for the SPI mission as the sail is jettisoned at the start of the science mission phase. As an alternative to conventional approaches, the micro-PPT-based ACS option promises lower mass, lower cost, and greater redundancy.

An attitude determination system (ADS), included in Fig. 10, is a critical subsystem of most spacecraft AOCS. An ADS of particular interest for solar-sail applications is the inertial stellar compass (ISC) recently developed by Draper Laboratory for an NMP ST6 flight validation experiment. The ISC is a miniature, low-power ADS developed for use with low-cost microsatellites. It is suitable for a wide range of future solar-sail missions because of its low-mass, low-power, and low-volume design and its self-initializing, autonomous operational capability. The ISC is composed of a wide field-of-view active-pixel star camera and microgyros, with associated data processing and power electronics. It has a total mass of 2.5 kg, a

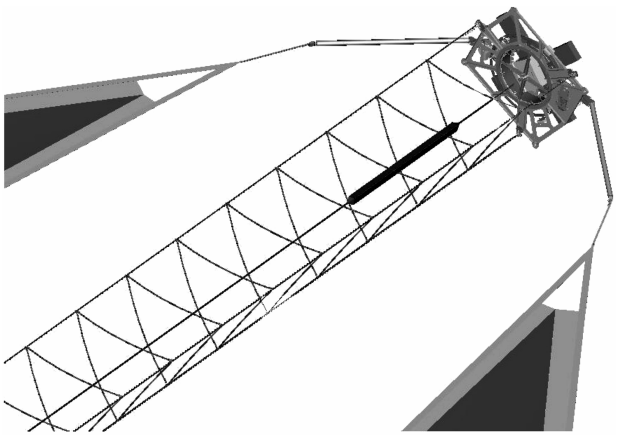

Fig. 11 ATK's solar-sail mast with a trim ballast mass running along a lanyard tape and tip-mounted roll stabilizer bars attached to sail panels (courtesy of ATK Space Systems).

power requirement of 3.5 W, and an accuracy of 0.1 deg (1σ). It is planned to be flight validated within a few years. Some recent advances in microsatellite technologies, including the ISC, need to be exploited to complete an integrated low-cost, low-risk, low-mass, low-power, and low-volume AOCS for sailcraft.

Detailed analysis and design of a similar TVC/AOCS architecture for a fight validation mission of a 40-m solar sail in a dawn–dusk sun-synchronous orbit can be found in [23–27]. The proposed baseline TVC/AOCS architecture will be applicable with minimal modifications to a wide range of future solar-sail flight missions with varying requirements and mission complexity, including a solar sailing mission for intercepting, impacting, and deflecting near-Earth asteroids [20,21]. Detailed control design study results of the proposed TVC/AOCS architecture for the SPI mission can be found in [28,29].

A navigation and guidance system, also included in Fig. 10, will also be required for most solar-sail missions. Because of the inherent inability to precisely model the solar radiation pressure and to accurately point the true thrust vector direction, most solar-sail TVC systems will require frequent updates of both orbital parameters and TVC steering commands for frequent trajectory corrections. The navigation and guidance system provides such required updates, and the update frequency is determined by many factors, such as the trajectory dispersions, the target-body ephemeris uncertainty, the calibration of a solar radiation pressure model, and the operational constraints. In [16] the interplanetary navigation problem of a solar-sail spacecraft was examined and found to be analogous to that of solar electric propulsion spacecraft. The study result in [16] also indicates that solar-sail spacecraft can be navigated without significant difficulties by applying techniques previously developed for solar electric propulsion missions. Although the development of a solar-sail navigation system is of practical importance for future solar-sail missions, this paper focuses on the TVC/AOCS design problem assuming that the navigation and guidance system can provide the required, frequent updates of both orbital parameters and TVC steering commands.

B. Quaternion-Feedback Attitude Control

Euler's attitude dynamical equations of motion of a rigid sailcraft are given by

$$I_1\dot{\omega}_1 - (I_2 - I_3)\omega_2\omega_3 = u_1 + d_1 \tag{26a}$$

$$I_2\dot{\omega}_2 - (I_3 - I_1)\omega_3\omega_1 = u_2 + d_2 \tag{26b}$$

$$I_3\dot{\omega}_3 - (I_1 - I_2)\omega_1\omega_2 = u_3 + d_3 \tag{26c}$$

where $(\omega_1, \omega_2, \omega_3)$ are the angular velocity components, (I_1, I_2, I_3) the principal moments of inertia, (u_1, u_2, u_3) the attitude control torques, and (d_1, d_2, d_3) the disturbance torques.

The kinematic differential equations in terms of attitude quaternions are given by

$$\begin{bmatrix} \dot{q}_1 \\ \dot{q}_2 \\ \dot{q}_3 \\ \dot{q}_4 \end{bmatrix} = \frac{1}{2}\begin{bmatrix} 0 & \omega_3 & -\omega_2 & \omega_1 \\ -\omega_3 & 0 & \omega_1 & \omega_2 \\ \omega_2 & -\omega_1 & 0 & \omega_3 \\ -\omega_1 & -\omega_2 & -\omega_3 & 0 \end{bmatrix}\begin{bmatrix} q_1 \\ q_2 \\ q_3 \\ q_4 \end{bmatrix} \tag{27}$$

where (q_1, q_2, q_3, q_4) are the inertial attitude quaternions.

The quaternion-feedback attitude control logic, proposed for solar sailing applications, is simply a proportional–integral–derivative (PID) control logic of the form [14,15,17]

$$u_1 = -k_1\left(e_1 + \frac{1}{\tau}\int e_1\,\mathrm{d}t\right) - c_1\omega_1 \tag{28a}$$

$$u_2 = -k_2\left(e_2 + \frac{1}{\tau}\int e_2\,\mathrm{d}t\right) - c_2\omega_2 \tag{28b}$$

$$u_3 = -k_3\left(e_3 + \frac{1}{\tau}\int e_3\,\mathrm{d}t\right) - c_3\omega_3 \tag{28c}$$

where (e_1, e_2, e_3) are the roll, pitch, and yaw components of attitude-error quaternions (e_1, e_2, e_3, e_4), and $(k_i, \tau, \mathrm{c}_i)$ are control gains to be properly determined. The attitude-error quaternions are computed using the desired or commanded attitude quaternions $(q_{1c}, q_{2c}, q_{3c}, q_{4c})$ and the actual attitude quaternions (q_1, q_2, q_3, q_4), as follows:

$$\begin{bmatrix} e_1 \\ e_2 \\ e_3 \\ e_4 \end{bmatrix} = \begin{bmatrix} q_{4c} & q_{3c} & -q_{2c} & -q_{1c} \\ -q_{3c} & q_{4c} & q_{1c} & -q_{2c} \\ q_{2c} & -q_{1c} & q_{4c} & -q_{3c} \\ q_{1c} & q_{2c} & q_{3c} & q_{4c} \end{bmatrix}\begin{bmatrix} q_1 \\ q_2 \\ q_3 \\ q_4 \end{bmatrix} \tag{29}$$

A saturation control logic accommodating the actuator torque and slew rate constraints is given by

$$u_i = -\mathrm{sat}_{U_{\max}}\left\{k_i\mathrm{sat}_{L_i}\left[e_i + \frac{1}{\tau}\int e_i\right] + c_i\omega_i\right\}; \qquad i = 1, 2, 3 \tag{30}$$

and the variable limiter L_i is self-adjusted as

$$L_i = \frac{c_i}{k_i}\min\{\sqrt{2a_i|e_i|}, \omega_{\max}\} \tag{31}$$

where $\omega_{\max}$ is the maximum slew rate (if required) and a_i is the maximum angular acceleration. Details of this nonlinear PID control logic can be found in [15,17].

C. Trajectory Control Inputs (α, β)

Consider the body-fixed rotational sequence of the form: $\mathbf{C}_2(-\alpha) \leftarrow \mathbf{C}_1(-\beta) \leftarrow \mathbf{C}_2(-\phi) \leftarrow \mathbf{C}_3(\psi)$. For this case of employing (α, β) as the trajectory control inputs or the TVC steering commands, we have

$$\begin{bmatrix} \hat{r} \\ \hat{\psi} \\ \hat{\phi} \end{bmatrix} = \begin{bmatrix} \cos\phi & 0 & \sin\phi \\ 0 & 1 & 0 \\ -\sin\phi & 0 & \cos\phi \end{bmatrix}\begin{bmatrix} \cos\psi & \sin\psi & 0 \\ -\sin\psi & \cos\psi & 0 \\ 0 & 0 & 1 \end{bmatrix}\begin{bmatrix} \hat{I} \\ \hat{J} \\ \hat{K} \end{bmatrix} \tag{32}$$

$$\begin{bmatrix} \hat{1} \\ \hat{2} \\ \hat{3} \end{bmatrix} = \begin{bmatrix} \cos\alpha & 0 & \sin\alpha \\ 0 & 1 & 0 \\ -\sin\alpha & 0 & \cos\alpha \end{bmatrix}\begin{bmatrix} 1 & 0 & 0 \\ 0 & \cos\beta & -\sin\beta \\ 0 & \sin\beta & \cos\beta \end{bmatrix}\begin{bmatrix} \hat{r} \\ \hat{\psi} \\ \hat{\phi} \end{bmatrix} \tag{33}$$

The equivalent coordinate transformation in terms of quaternions is expressed as [17]

$$\begin{bmatrix} 0 \\ -\sin(\alpha/2) \\ 0 \\ \cos(\alpha/2) \end{bmatrix} \leftarrow \begin{bmatrix} -\sin(\beta/2) \\ 0 \\ 0 \\ \cos(\beta/2) \end{bmatrix} \leftarrow \begin{bmatrix} 0 \\ -\sin(\phi/2) \\ 0 \\ \cos(\phi/2) \end{bmatrix} \leftarrow \begin{bmatrix} 0 \\ 0 \\ \sin(\psi/2) \\ \cos(\psi/2) \end{bmatrix} \tag{34}$$

which results in

$$\begin{bmatrix} q_{1c} \\ q_{2c} \\ q_{3c} \\ q_{4c} \end{bmatrix} = \begin{bmatrix} \cos(\alpha/2) & 0 & \sin(\alpha/2) & 0 \\ 0 & \cos(\alpha/2) & 0 & -\sin(\alpha/2) \\ -\sin(\alpha/2) & 0 & \cos(\alpha/2) & 0 \\ 0 & \sin(\alpha/2) & 0 & \cos(\alpha/2) \end{bmatrix} \times \begin{bmatrix} \cos(\beta/2) & 0 & 0 & -\sin(\beta/2) \\ 0 & \cos(\beta/2) & -\sin(\beta/2) & 0 \\ 0 & \sin(\beta/2) & \cos(\beta/2) & 0 \\ \sin(\beta/2) & 0 & 0 & \cos(\beta/2) \end{bmatrix} \times \begin{bmatrix} \cos(\phi/2) & 0 & \sin(\phi/2) & 0 \\ 0 & \cos(\phi/2) & 0 & -\sin(\phi/2) \\ -\sin(\phi/2) & 0 & \cos(\phi/2) & 0 \\ 0 & \sin(\phi/2) & 0 & \cos(\phi/2) \end{bmatrix} \begin{bmatrix} 0 \\ 0 \\ \sin(\psi/2) \\ \cos(\psi/2) \end{bmatrix} \tag{35}$$

where $(q_{1c}, q_{2c}, q_{3c}, q_{4c})$ are the desired attitude quaternions of a sailcraft whose orientation provides the desired thrust vector direction as commanded by (α, β). The preceding result indicates that a TVC system will require frequent updates of both the orbital information (ϕ, ψ) and TVC steering commands (α, β) due to the inherent difficulty to precisely point the true thrust vector of a large solar sail.

Given the actual attitude quaternions, (q_1, q_2, q_3, q_4), the actual cone and clock angles (α, β) can be determined from the following relationship:

$$\begin{bmatrix} 1-2(q_2^2+q_3^2) & 2(q_1q_2+q_3q_4) & 2(q_1q_3-q_2q_4) \\ 2(q_2q_1-q_3q_4) & 1-2(q_1^2+q_3^2) & 2(q_2q_3+q_1q_4) \\ 2(q_3q_1+q_2q_4) & 2(q_3q_2-q_1q_4) & 1-2(q_1^2+q_2^2) \end{bmatrix} = \begin{bmatrix} C_{11} & C_{12} & C_{13} \\ C_{21} & C_{22} & C_{23} \\ C_{31} & C_{32} & C_{33} \end{bmatrix} = \begin{bmatrix} \cos\alpha & 0 & \sin\alpha \\ 0 & 1 & 0 \\ -\sin\alpha & 0 & \cos\alpha \end{bmatrix} \begin{bmatrix} 1 & 0 & 0 \\ 0 & \cos\beta & -\sin\beta \\ 0 & \sin\beta & \cos\beta \end{bmatrix} \times \begin{bmatrix} \cos\phi & 0 & \sin\phi \\ 0 & 1 & 0 \\ -\sin\phi & 0 & \cos\phi \end{bmatrix} \begin{bmatrix} \cos\psi & \sin\psi & 0 \\ -\sin\psi & \cos\psi & 0 \\ 0 & 0 & 1 \end{bmatrix}$$

Given a direction cosine matrix, quaternions can also be determined as

$$q_4 = \frac{1}{2}\sqrt{1 + C_{11} + C_{22} + C_{33}}$$

$$\begin{bmatrix} q_1 \\ q_2 \\ q_3 \end{bmatrix} = \frac{1}{4q_4} \begin{bmatrix} C_{23} - C_{32} \\ C_{31} - C_{13} \\ C_{12} - C_{21} \end{bmatrix}; \quad \text{when } q_4 \neq 0$$

However, this approach has a singularity problem when $q_4 = 0$.

D. Trajectory Control Inputs (α, δ)

For a case of employing (α, δ) as the trajectory control inputs or the TVC steering commands, consider a body-fixed rotational sequence of the form: $\mathbf{C}_2(-\alpha) \leftarrow \mathbf{C}_1(-\delta) \leftarrow \mathbf{C}_3(\theta) \leftarrow \mathbf{C}_3(\omega) \leftarrow \mathbf{C}_1(i) \leftarrow \mathbf{C}_3(\Omega)$. For this case, we have

$$\begin{bmatrix} \hat{r} \\ \hat{\theta} \\ \hat{k} \end{bmatrix} = \begin{bmatrix} \cos(\omega+\theta) & \sin(\omega+\theta) & 0 \\ -\sin(\omega+\theta) & \cos(\omega+\theta) & 0 \\ 0 & 0 & 1 \end{bmatrix} \begin{bmatrix} 1 & 0 & 0 \\ 0 & \cos i & \sin i \\ 0 & -\sin i & \cos i \end{bmatrix} \times \begin{bmatrix} \cos\Omega & \sin\Omega & 0 \\ -\sin\Omega & \cos\Omega & 0 \\ 0 & 0 & 1 \end{bmatrix} \begin{bmatrix} \hat{I} \\ \hat{J} \\ \hat{K} \end{bmatrix} \tag{36}$$

$$\begin{bmatrix} \hat{1} \\ \hat{2} \\ \hat{3} \end{bmatrix} = \begin{bmatrix} \cos\alpha & 0 & \sin\alpha \\ 0 & 1 & 0 \\ -\sin\alpha & 0 & \cos\alpha \end{bmatrix} \begin{bmatrix} 1 & 0 & 0 \\ 0 & \cos\delta & -\sin\delta \\ 0 & \sin\delta & \cos\delta \end{bmatrix} \begin{bmatrix} \hat{r} \\ \hat{\theta} \\ \hat{k} \end{bmatrix} \tag{37}$$

$$\begin{bmatrix} 0 \\ -\sin(\alpha/2) \\ 0 \\ \cos(\alpha/2) \end{bmatrix} \leftarrow \begin{bmatrix} -\sin(\delta/2) \\ 0 \\ 0 \\ \cos(\delta/2) \end{bmatrix} \leftarrow \begin{bmatrix} 0 \\ 0 \\ \sin\left(\frac{\omega+\theta}{2}\right) \\ \cos\left(\frac{\omega+\theta}{2}\right) \end{bmatrix} \leftarrow \begin{bmatrix} \sin(i/2) \\ 0 \\ 0 \\ \cos(i/2) \end{bmatrix} \leftarrow \begin{bmatrix} 0 \\ 0 \\ \sin(\Omega/2) \\ \cos(\Omega/2) \end{bmatrix} \tag{38}$$

$$\begin{bmatrix} q_{1c} \\ q_{2c} \\ q_{3c} \\ q_{4c} \end{bmatrix} = \begin{bmatrix} \cos(\alpha/2) & 0 & \sin(\alpha/2) & 0 \\ 0 & \cos(\alpha/2) & 0 & -\sin(\alpha/2) \\ -\sin(\alpha/2) & 0 & \cos(\alpha/2) & 0 \\ 0 & \sin(\alpha/2) & 0 & \cos(\alpha/2) \end{bmatrix} \times \begin{bmatrix} \cos(\delta/2) & 0 & 0 & -\sin(\delta/2) \\ 0 & \cos(\delta/2) & -\sin(\delta/2) & 0 \\ 0 & \sin(\delta/2) & \cos(\delta/2) & 0 \\ \sin(\delta/2) & 0 & 0 & \cos(\delta/2) \end{bmatrix} \times \begin{bmatrix} \cos\left(\frac{\omega+\theta}{2}\right) & \sin\left(\frac{\omega+\theta}{2}\right) & 0 & 0 \\ -\sin\left(\frac{\omega+\theta}{2}\right) & \cos\left(\frac{\omega+\theta}{2}\right) & 0 & 0 \\ 0 & 0 & \cos\left(\frac{\omega+\theta}{2}\right) & \sin\left(\frac{\omega+\theta}{2}\right) \\ 0 & 0 & -\sin\left(\frac{\omega+\theta}{2}\right) & \cos\left(\frac{\omega+\theta}{2}\right) \end{bmatrix} \times \begin{bmatrix} \cos(i/2) & 0 & 0 & \sin(i/2) \\ 0 & \cos(i/2) & \sin(i/2) & 0 \\ 0 & -\sin(i/2) & \cos(i/2) & 0 \\ -\sin(i/2) & 0 & 0 & \cos(i/2) \end{bmatrix} \begin{bmatrix} 0 \\ 0 \\ \sin(\Omega/2) \\ \cos(\Omega/2) \end{bmatrix} \tag{39}$$

The preceding result indicates that a TVC system employing (α, δ) will also require frequent updates of both the orbital parameters $(\Omega, i, \omega, \theta)$ and TVC steering commands (α, δ) due to the inherent inability to point the true thrust vector direction of a large solar sail.

Equation (39) provides a simple computational algorithm for determining the desired attitude quaternions from the commanded cone/clock angles (α, δ).

Given the actual attitude quaternions (q_1, q_2, q_3, q_4), the actual cone and clock angles (α, δ) can be determined from the following relationship:

$$\begin{bmatrix} 1-2(q_2^2+q_3^2) & 2(q_1q_2+q_3q_4) & 2(q_1q_3-q_2q_4) \\ 2(q_2q_1-q_3q_4) & 1-2(q_1^2+q_3^2) & 2(q_2q_3+q_1q_4) \\ 2(q_3q_1+q_2q_4) & 2(q_3q_2-q_1q_4) & 1-2(q_1^2+q_2^2) \end{bmatrix} = \begin{bmatrix} \cos\alpha & 0 & \sin\alpha \\ 0 & 1 & 0 \\ -\sin\alpha & 0 & \cos\alpha \end{bmatrix} \begin{bmatrix} 1 & 0 & 0 \\ 0 & \cos\delta & -\sin\delta \\ 0 & \sin\delta & \cos\delta \end{bmatrix} \times \begin{bmatrix} \cos(\omega+\theta) & \sin(\omega+\theta) & 0 \\ -\sin(\omega+\theta) & \cos(\omega+\theta) & 0 \\ 0 & 0 & 1 \end{bmatrix} \begin{bmatrix} 1 & 0 & 0 \\ 0 & \cos i & \sin i \\ 0 & -\sin i & \cos i \end{bmatrix} \times \begin{bmatrix} \cos\Omega & \sin\Omega & 0 \\ -\sin\Omega & \cos\Omega & 0 \\ 0 & 0 & 1 \end{bmatrix} \tag{40}$$

E. Relationship of β and δ

The two different clock angles β and δ are related as

$$\begin{bmatrix} 1 & 0 & 0 \\ 0 & \cos\beta & -\sin\beta \\ 0 & \sin\beta & \cos\beta \end{bmatrix} \begin{bmatrix} \cos\phi & 0 & \sin\phi \\ 0 & 1 & 0 \\ -\sin\phi & 0 & \cos\phi \end{bmatrix} \begin{bmatrix} \cos\psi & \sin\psi & 0 \\ -\sin\psi & \cos\psi & 0 \\ 0 & 0 & 1 \end{bmatrix}$$
$$= \begin{bmatrix} 1 & 0 & 0 \\ 0 & \cos\delta & -\sin\delta \\ 0 & \sin\delta & \cos\delta \end{bmatrix} \begin{bmatrix} \cos(\omega+\theta) & \sin(\omega+\theta) & 0 \\ -\sin(\omega+\theta) & \cos(\omega+\theta) & 0 \\ 0 & 0 & 1 \end{bmatrix}$$
$$\times \begin{bmatrix} 1 & 0 & 0 \\ 0 & \cos i & \sin i \\ 0 & -\sin i & \cos i \end{bmatrix} \begin{bmatrix} \cos\Omega & \sin\Omega & 0 \\ -\sin\Omega & \cos\Omega & 0 \\ 0 & 0 & 1 \end{bmatrix}$$

V. TVC Design and Simulation for the SPI Mission

A. Simplified Control Design Model

Although various forms of orbital trajectory equations employing two different sets of the cone and clock angles are available for the solar-sail trajectory design and simulation, we choose here a set of orbital equations, called Gauss's form of the variational equations with (α, δ), for the preliminary TVC design and simulation.

A dynamic model of sailcraft with a trim control mass (TCM) translating along the yaw axis to generate a pitch control torque is illustrated in Fig. 12. A set of simplified attitude equations of motion are considered for control design, as follows:

$$J_1\dot{\omega}_1 = u_1 + d_1 \tag{41}$$

$$J_2\dot{\omega}_2 = u_2 + d_2 \tag{42}$$

$$J_3\dot{\omega}_3 = u_3 + d_3 \tag{43}$$

$$u_1 = C\sin\Theta$$

$$u_2 = -\frac{m_r F}{(M+m)}z$$

$$u_3 = \frac{m_r F}{(M+m)}y$$

$$d_1 = \pm 0.5\epsilon F, \qquad d_2 = d_3 = \pm\epsilon F$$

$$J_1 = I_1 + m_r(y^2 + z^2)$$

$$J_2 = I_2 + m_r z^2$$

$$J_3 = I_3 + m_r y^2$$

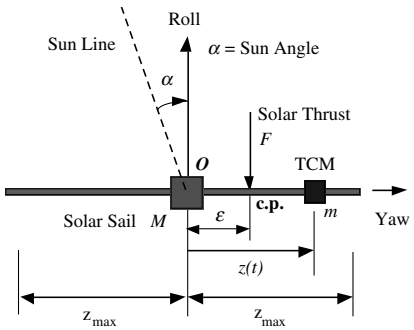

Fig. 12 A dynamic model of sailcraft with a trim control mass moving along the yaw axis to generate a pitch control torque.

where Θ is the RSB tilt angle, C is the RSB control scale factor, y and z are the TCM positions along the pitch and yaw axes, respectively, F is the solar radiation pressure force defined as

$$F \approx \left(\frac{r_\oplus}{r}\right)^2 F_s\cos^2\alpha = 2\eta PA\left(\frac{r_\oplus}{r}\right)^2\cos^2\alpha \tag{44}$$

and m_r is the so-called reduced mass defined as

$$m_r = \frac{m(M+m)}{M+2m} \tag{45}$$

Note that $m_r \approx m$ because $M \gg m$.

A reference 160-m SPI sailcraft model for TVC/AOCS design is assumed as follows [28]:

sail size = 160 m × 160 m;
scallop factor = 75%;
sail area $A = 19,200$ m^2 with $\eta = 0.84$;
solar thrust force $F_s = 0.16$ N (at 1 AU), 0.69 N (at 0.48 AU);
sailcraft total mass = 450 kg (150-kg sail, 250-kg bus, and 50-kg payload);
characteristic acceleration $a_c = 0.35$ mm/s^2 (at 1 AU);
moments of inertia $(I_1, I_2, I_3) = (642,876,\ 321,490,\ 321,490)$ kg · m^2
c.m./c.p. offset $\epsilon = 0.4$ m (0.25% of 160 m)
disturbance torque = 0.064 N · m (1 AU), 0.256 N · m (at 0.48 AU);
trim control mass $m = 5$ kg (each axis);
main-body mass $M = 440$ kg;
TCM speed limit = 5 cm/s;
TCM $y_{\max} = z_{\max} = \pm 100$ m;
RSB maximum deflection angle $\Theta_{\max} = \pm 45$ deg;
RSB moment arm length = 1.7 m;
$(a, e, i, \Omega, \omega, \theta) = (0.48$ AU, $1E\text{-}5, 45$ deg, $0, 0, 0)$ at $t = 0$.

B. Roll-Axis Control Design

The roll-axis control logic is assumed as

$$u_1 = -\text{sat}_{U_{\max}}\left\{K_1\text{sat}_{L_1}\left[e_1 + \frac{1}{\tau_i}\int e_1\,\mathrm{d}t\right] + D_1\omega_1\right\} \tag{46}$$

where u_1 is the roll control torque command with a saturation limit of $U_{\max} = C\sin\Theta_{\max}$ and the variable limiter L_1 is self-adjusted as

$$L_1 = \frac{C_1}{D_1}\min\{\sqrt{2a_1|e_1|}, \omega_{\max}\} \tag{47}$$

where $a_1 = U_{\max}/J_1$ and $\omega_{\max}$ is assumed to be constrained as 0.1 deg/s.

The roll control torque u_1 (in units of N · m) is related to the tilt angle Θ of the RSB of an assumed moment arm length of 1.7 m for a 160-m sailcraft, as follows:

$$u_1 = C\sin\Theta \approx \frac{(1.7)(53.2)}{80}F\sin\Theta \tag{48}$$

It is assumed that all four RSBs are rotated simultaneously. Consequently, we have $U_{\max}$ of ± 0.15 N · m (at 1 AU) for a maximum tilt angle of ± 45 deg.

The RSB actuator dynamics is also assumed as

$$T\dot{\Theta} + \Theta = \Theta_c; \qquad |\Theta_c(t)| \le \Theta_{\max} \tag{49}$$

where T is the actuator time constant, Θ is the actual tilt angle, and Θ_c is the commanded tilt angle (the control input) with a maximum value of $\Theta_{\max}$. The commanded tilt angle of the RSB is then given by

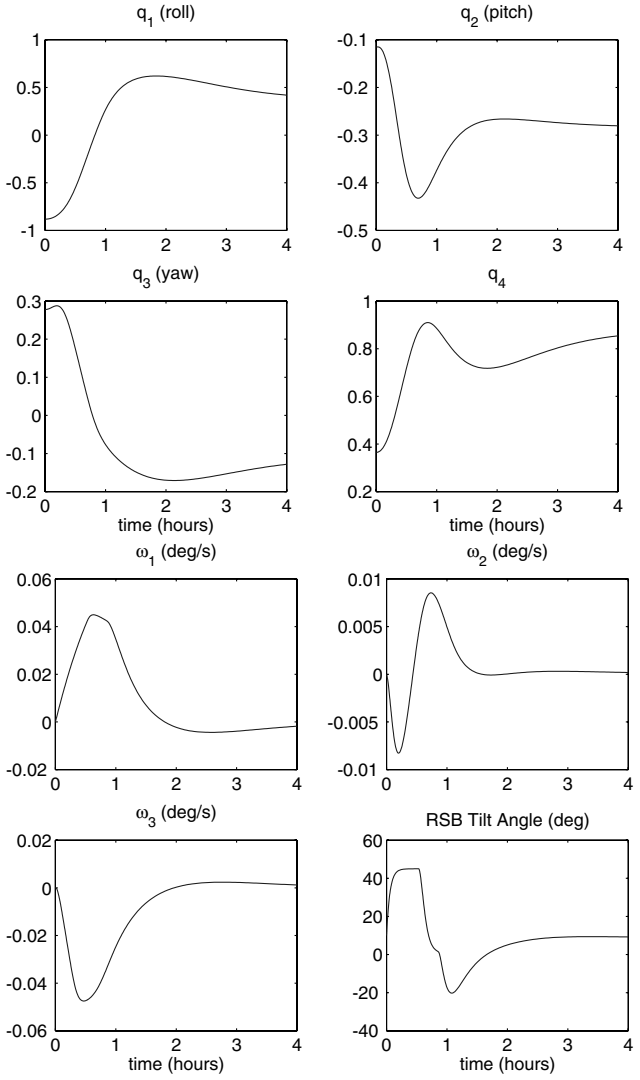

Fig. 13 A 180-deg δ clock-angle maneuver with a fixed 35-deg cone-angle command.

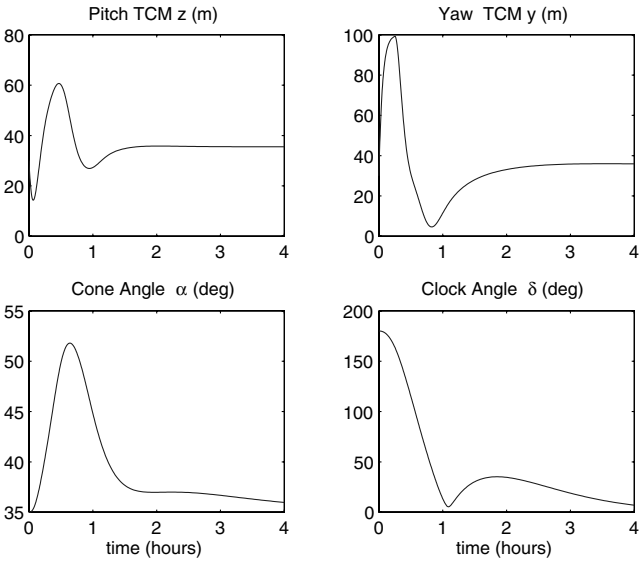

Fig. 14 A 180-deg δ clock-angle maneuver with a fixed 35-deg cone-angle command.

$$\Theta_c = \arcsin\left\{\frac{80u_1}{(1.7)(53.2)F}\right\} \approx \frac{80u_1}{(1.7)(53.2)F} \tag{50}$$

where

$$F \approx 0.16\left(\frac{r_\oplus}{r}\right)^2 \cos^2\alpha \tag{51}$$

and u_1 is given by Eq. (46).

C. Pitch/Yaw Control Design

The steady-state trim position of the pitch TCM for countering the effect of the c.m./c.p. offset ϵ can be estimated as

$$z_{ss} = \frac{(M+m)}{m_r}\epsilon \approx \frac{(M+m)}{m}\epsilon = \pm 35 \text{ m} \tag{52}$$

The actuator dynamics of the pitch TCM is assumed as

$$T\dot{z} + z = z_c; \qquad |z_c(t)| \le z_{\max} \tag{53}$$

where T is the actuator time constant, z is the actual position, and z_c is the commanded position (the control input) with a maximum value of $z_{\max}$. For a reference control design, it is assumed that $z_{\max} = \pm 100$ m, $\dot{z}_{\max} = \pm 0.05$ m/s, and $T = 200$ s for a 160-m sailcraft with $M = 440$ kg, $m = 5$ kg, and $\epsilon = \pm 0.4$ m.

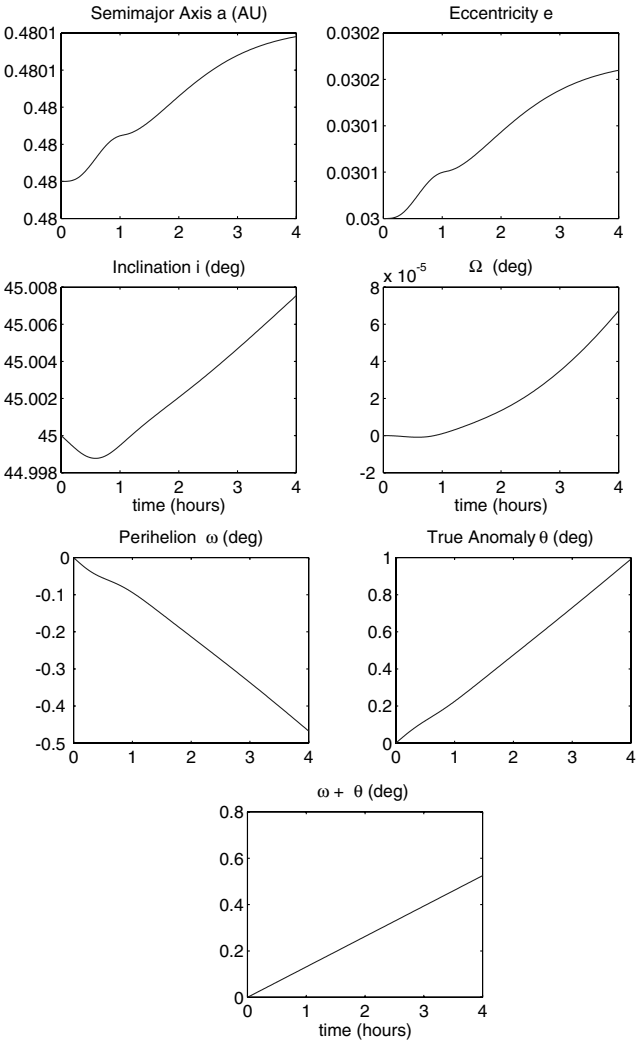

Fig. 15 A 180-deg δ clock-angle maneuver with a fixed 35-deg cone-angle command.

The pitch control logic is assumed as

$$z_c = \text{sat}_{z_{\max}}\left\{K_2 \text{sat}_{L_2}\left[e_2 + \frac{1}{\tau_2}\int e_2\,\mathrm{d}t\right] + D_2\omega_2\right\} \tag{54}$$

where τ is the time constant of integral control and variable limiter L_2 is self-adjusted as

$$L_2 = \frac{D_2}{K_2}\min\left\{\sqrt{2a_2|e_2|}, \omega_{\max}\right\} \tag{55}$$

Similarly, we have the yaw control logic as

$$y_c = -\text{sat}_{y_{\max}}\left\{K_3 \text{sat}_{L_3}\left[e_3 + \frac{1}{\tau_3}\int e_3\,\mathrm{d}t\right] + D_3\omega_3\right\} \tag{56}$$

where $y_{\max} = \pm 100$ m.

D. Simulation Example: Cranking Orbit Phase at 0.48 AU

An attitude maneuver for achieving a desired 180-deg δ clock-angle change within 3 h (with a fixed cone-angle command of 35 deg) is illustrated in Figs. 13–15. An equivalent, direct 70-deg pitch maneuver within 3 h was also validated but not included here. An inclination increase of 0.06 deg/day can be seen in Fig. 16 for the cranking orbit phase of the SPI mission. The robustness of a propellantless primary ACS described in this section can be further enhanced by a secondary ACS using tip-mounted, lightweight PPTs.

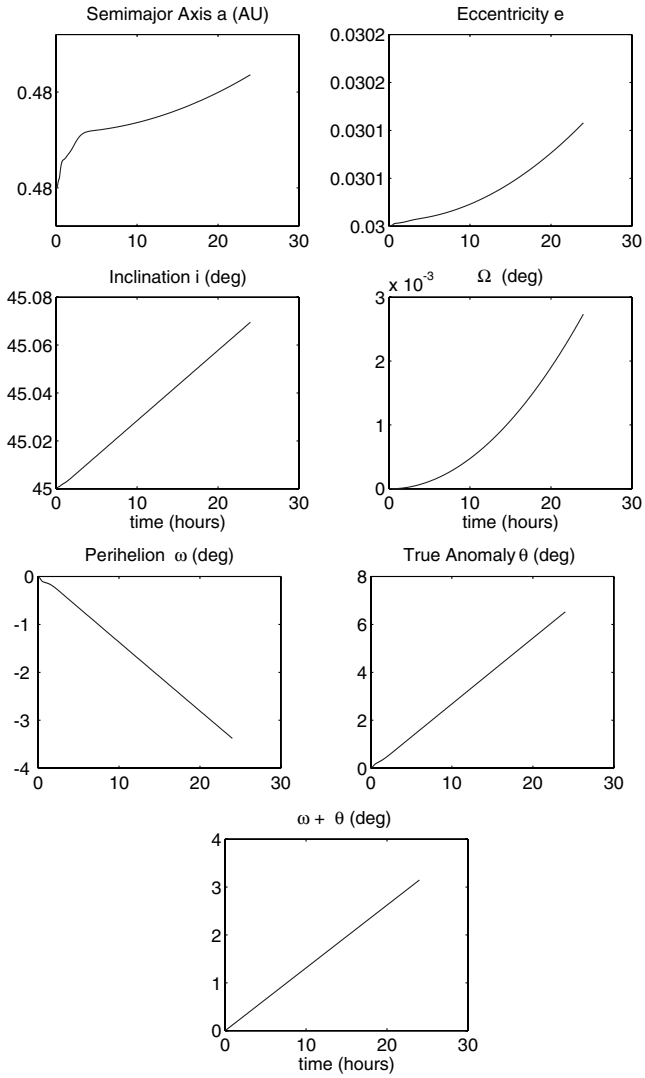

Fig. 16 Twenty-four hour simulation showing a 0.06-deg inclination increase per day.

The micro-PPT-based ACS is mainly intended for attitude recovery maneuvers from off-nominal conditions. Details of the ACS design and simulation for the SPI mission can be found in [28,29].

VI. Conclusions

This paper has described various forms of orbital trajectory equations, which employ two different sets of the cone and clock angles, for the TVC design and simulation of a solar-sail spacecraft. It was shown that a preliminary trajectory design can be easily performed by employing simple sail-steering laws as applied to a set of orbital equations, called Gauss's form of the variational equations of sailcraft whose thrust vector direction is measured by its cone and clock angles (α, δ). The simplicity of a quaternion-based TVC/AOCS architecture was demonstrated. However, most solar-sail TVC systems will require frequent updates of both the TVC steering commands (α, δ) and orbital parameters because of its inability to precisely point the true thrust vector direction of a large flexible solar sail. Consequently, the proposed simple computational algorithm for determining the desired attitude quaternions from the commanded cone/clock angles (α, δ) will become more useful in such practical situations requiring frequent updates of both the TVC steering commands and orbital parameters.

Acknowledgments

This work was funded by the In-Space Propulsion Technology Program, which is managed by NASA's Science Mission Directorate in Washington, D.C., and implemented by the In-Space Propulsion Technology Office at Marshall Space Flight Center in Huntsville, Alabama. The program objective is to develop in-space propulsion technologies that can enable or benefit near and midterm NASA space science missions by significantly reducing cost, mass, or travel times. The author would like to thank E. Montgomery, G. Garbe, J. Presson, A. Heaton, and M. Whorton at NASA Marshall Space Flight Center for their financial and technical support.

References

[1] Wright, J. L., *Space Sailing*, Gordon and Breach, New York, 1992.
[2] McInnes, C. R., *Solar Sailing: Technology, Dynamics and Mission Applications*, Springer Praxis Publishing, Chichester, U.K., 1999.
[3] Garbe, G., and Montgomery, E., "An Overview of NASA's Solar Sail Propulsion Project," AIAA Paper 2003-4662, 2003.
[4] Murphy, D. M., McEachen, M. E., Macy, B. D., and Gaspar, J. L., "Demonstration of a 20-m Solar Sail System," AIAA Paper 2005-2126, 2005.
[5] Lichodziejewski, D., Derbès, B., Slade, K., and Mann, T., "Vacuum Deployment and Testing of a 4-Quadrant Scalable Inflatable Rigidizable Solar Sail System," AIAA Paper 2005-3927, 2005.
[6] Sauer, C., "A Comparison of Solar Sail and Ion Drive Trajectories for a Halley's Comet Rendezvous Mission," AAS Paper 77-104, 1977.
[7] Hur, S.-H., and Bryson, A. E., "Minimum Time Solar Sailing from Geosynchronous Orbit to the Sun-Earth L_2 Point," AIAA Paper 1992-4657, 1992.
[8] Sauer, C., Solar Sail Trajectories for Solar Polar and Interstellar Probe Mission, *Advances in the Astronautical Sciences*, Univelt, Inc., San Diego, CA, Vol. 103, 2000, pp. 547–562.
[9] Coverstone-Carroll, V. L., and Prussing, J. E., "Technique for Escape from Geosynchronous Transfer Orbit Using a Solar Sail," *Journal of Guidance, Control, and Dynamics*, Vol. 26, No. 4, 2003, pp. 628–634.
[10] Yen, C.-W., "Solar Sail Geostorm Mission," AAS Paper 04-107, 2004.
[11] Sauer, C. G., "The L1-Diamond Affair," AAS Paper 04-278, 2004.
[12] Dachwald, B., "Optimal Solar Sail Trajectories for Missions to the Outer Solar System," *Journal of Guidance, Control, and Dynamics*, Vol. 28, No. 6, 2005, pp. 1187–1193.
[13] Lisano, M. E., "A Practical Six-Degree-of-Freedom Solar Sail Dynamics Model for Optimizing Solar Sail Trajectories with Torque Constraints," AIAA Paper 2004-4891, 2004.
[14] Wie, B., and Barba, P. M., "Quaternion Feedback for Spacecraft Large Angle Maneuvers," *Journal of Guidance, Control, and Dynamics*, Vol. 8, No. 3, 1985, pp. 360–365.
[15] Wie, B., Heiberg, C., and Bailey, D., "Rapid Multi-Target Acquisition and Pointing Control of Agile Spacecraft," *Journal of Guidance, Control, and Dynamics*, Vol. 25, No. 1, 2002, pp. 96–104.

[16] Jacobson, R., and Thornton, C.,"Elements of Solar Sail Navigation with Application to a Halley's Comet Rendezvous," *Journal of Guidance and Control*, Vol. 1, No. 5, 1978, pp. 365–371.
[17] Wie, B., *Space Vehicle Dynamics and Control*, AIAA Education Series, AIAA, Reston, VA, 1998, Chaps. 3, 5.
[18] Bacon, R. H., "Logarithmic Spiral—An Ideal Trajectory for an Interplanetary Vehicle with Engines of Low Sustained Thrust," *American Journal of Physics*, Vol. 27, No. 3, 1959, pp. 12–18.
[19] Battin, R. H., *An Introduction to the Mathematics and Methods of Astrodynamics*, AIAA Education Series, AIAA, New York, 1987.
[20] Wie, B., "Solar Sailing Kinetic Energy Interceptor (KEI) Mission for Impacting and Deflecting Near-Earth Asteroids," AIAA Paper 2005-6175, 2005.
[21] Dachwald, B., and Wie, B., "Solar Sail Trajectory Optimization for Intercepting, Impacting, and Deflecting Near-Earth Asteroids," AIAA Paper 2005-6176, 2005, *Journal of Spacecraft and Rockets* (submitted for publication).
[22] Wie, B., "Solar Sail Attitude Control and Dynamics, Parts 1 and 2," *Journal of Guidance, Control, and Dynamics*, Vol. 27, No. 4, 2004, pp. 526–544.
[23] Murphy, D., and Wie, B., "Robust Thrust Control Authority for a Scalable Sailcraft," AAS Paper 04-285, 2004.
[24] Wie, B., Murphy, D., Thomas, S., and Paluszek, M., "Robust Attitude Control Systems Design for Solar Sail Spacecraft (Part 1): Propellantless Primary ACS," AIAA Paper 2004-5010, 2004.
[25] Wie, B., Murphy, D., Thomas, S., and Paluszek, M., "Robust Attitude Control Systems Design for Solar Sail Spacecraft (Part 2): MicroPPT-Based Backup ACS," AIAA Paper 2004-5011, 2004.
[26] Thomas, S., Paluszek, M., Wie, B., and Murphy, D., "Design and Simulation of Sailcraft Attitude Control Systems Using Solar Sail Control Toolbox," AIAA Paper 2004-4890, 2004.
[27] Wie, B., and Murphy, D., "Solar-Sail ACS Development for a Sail Flight Validation Mission in a Sun-Synchronous Orbit," *Journal of Spacecraft and Rockets* (submitted for publication).
[28] Wie, B., Thomas, S., Paluszek, M., and Murphy, D., "Propellantless AOCS Design for a 160-m, 450-kg Solar Sail Spacecraft of the Solar Polar Imager Mission," AIAA Paper 2005-3928, 2005.
[29] Wie, B., and Murphy, D., "MicroPPT-Based Secondary/Backup ACS for a 160-m, 450-kg Solar Sail Spacecraft," AIAA Paper 2005-3724, 2005.

R. Braun
Associate Editor